Science Advances
AAAS

Supplementary Materials for

LHX2 regulates dendritic morphogenesis in layer II/III neurons of the neocortex

Mahima Bose *et al.*

Corresponding author: Shubha Tole, shubhatole@gmail.com

Sci. Adv. **11**, eado1384 (2025)
DOI: 10.1126/sciadv.ado1384

The PDF file includes:

Figs. S1 to S10
Legends for datasets S1 to S3

Other Supplementary Material for this manuscript includes the following:

Datasets S1 to S3

Fig. S1.

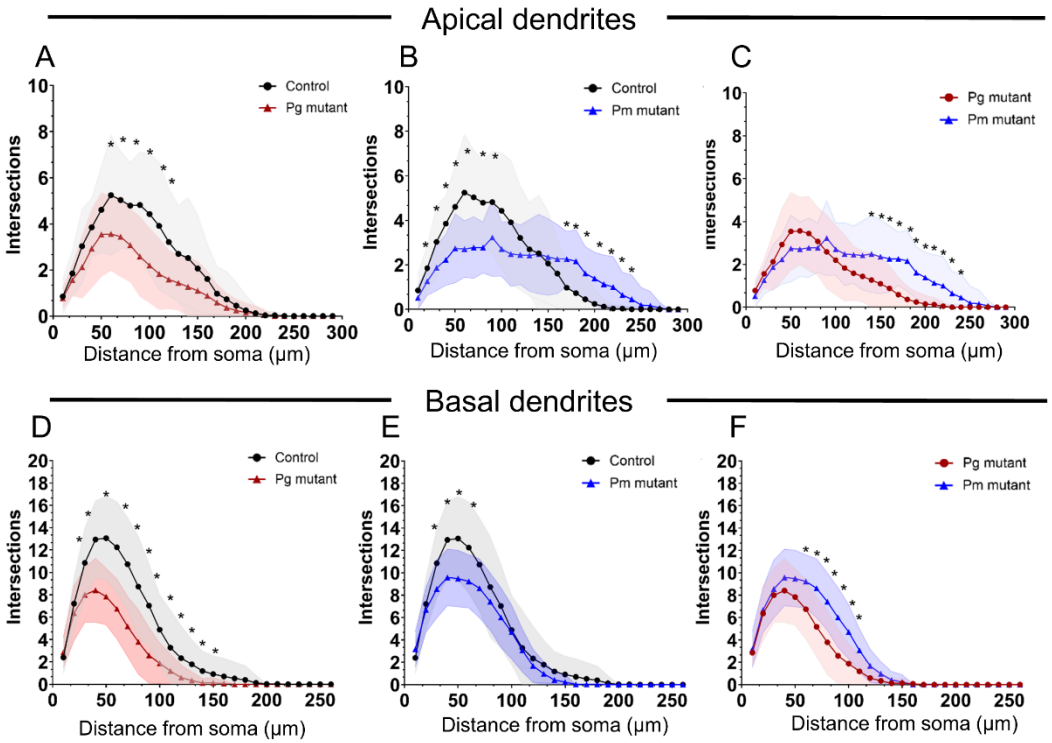

Supplementary Figure S1: Progenitor and postmitotic loss of *Lhx2* lead to distinct levels of dendritic complexity defects.

Pairwise comparisons between Control (black line), Pg mutant (red line), and Pm mutant (blue line) apical dendrite (A–C) and basal dendrite (D–F) complexities with asterisks marking significant differences as shown in Figure 1H, I. 35 to 40 neurons were scored for each condition obtained from 4 biologically independent replicates; *Statistical test: Multiple T Tests (two-tailed). *(p<0.05).*

Fig. S2

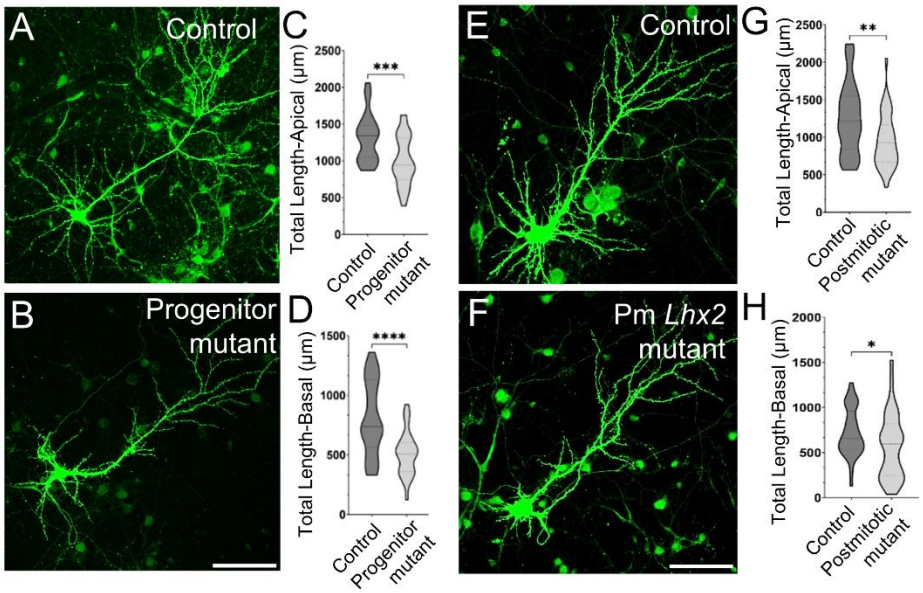

Supplementary Figure S2: Dissociated primary cultures of Pg and Pm neurons recapitulate *in vivo* phenotypes.

(A–D) Representative images and quantification of control (A) and Pg mutant (B) neurons cultured for 15 days *in vitro* (DIV). Pg mutant neurons exhibit a significant reduction in total apical (C) and basal (D) dendritic length compared to controls. (E–H) Representative images and quantification of control (E) and Pm mutant (F) neurons cultured for 15 DIV. Pm mutant neurons similarly show a significant reduction in total apical (G) and basal (H) dendritic length compared to controls.

Fig. S3

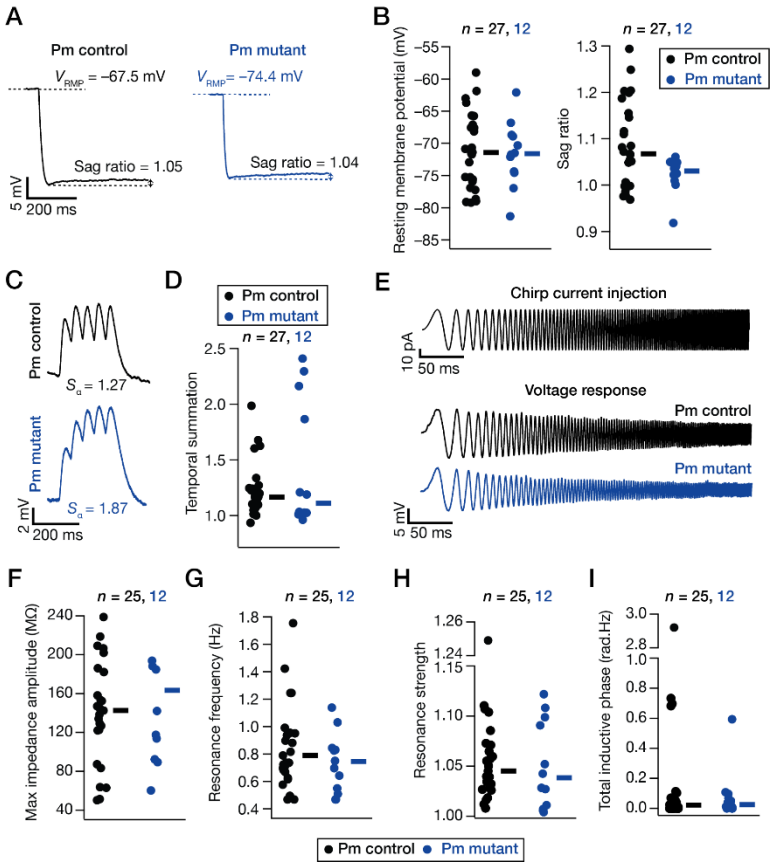

Supplementary Figure S3: Sub-threshold measurements for neocortical layer II/III pyramidal neurons from control and postmitotic (Pm) *Lhx2* mutant groups.

(A) Traces showing voltage response to a 250-pA hyperpolarising pulse current for the example control (left) and Pm mutant (right) neurons. The resting membrane potential (V_{RMP}) is shown with a dotted line on top of the trace just before the current injection. Sag is represented as the difference between the initial peak and the steady-state voltage deflection. (B) Beeswarm plots of resting membrane potential (V_{RMP}) (left) and Sag ratio (right) recorded from all control and Pm mutant neurons. (C) Train of five excitatory postsynaptic potentials (α-EPSPs) recorded from example control (top) and Pm mutant (bottom) neurons. Temporal summation (S_α) was calculated as a ratio between the last and the first EPSP amplitudes. (D) Beeswarm of S_α recorded from all control and Pm mutant neurons. (E) *Top*, Chirp current stimulus. *Bottom*, Voltage responses of the example control and mutant neurons to the chirp current stimulus. (F–I) Beeswarm plots of maximum impedance amplitude (F), resonance frequency, f_R (G), resonance strength, Q (H), and total inductive phase, ϕ_L (I) calculated for all control and Pm mutant neurons. *Statistical test: Wilcoxon rank sum test. n represents the number of total neurons recorded in each group. The thick line on the right of each beeswarm plot depicts respective median values.*

Fig. S4

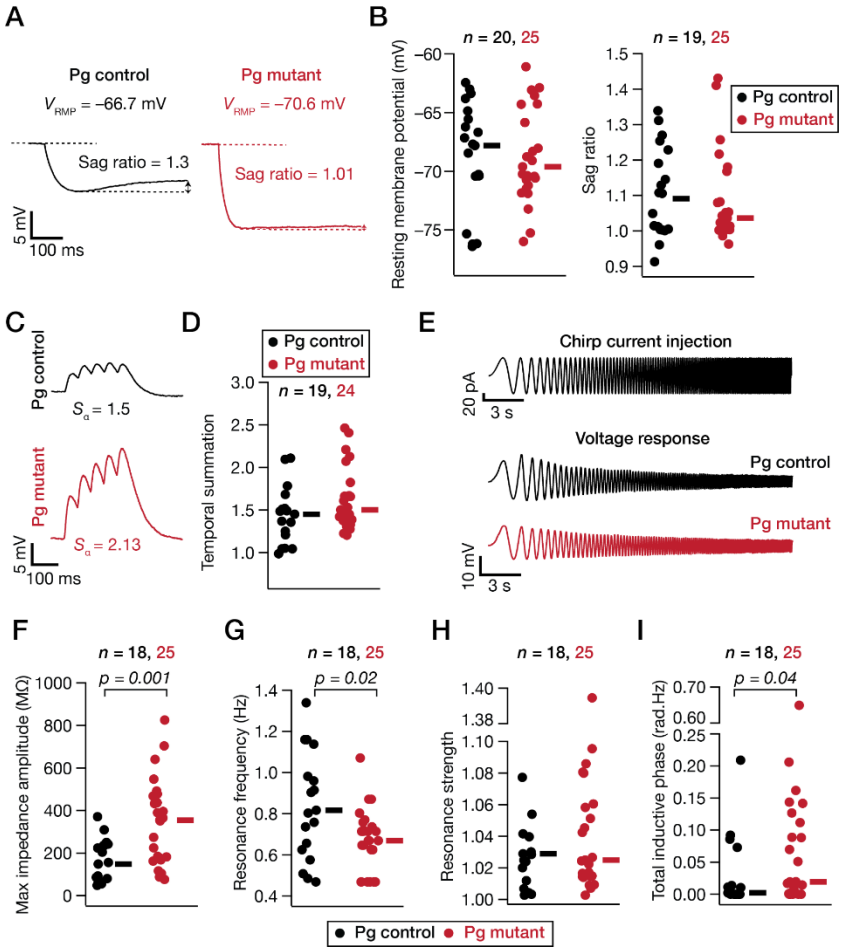

Supplementary Figure S4: Sub-threshold measurements for neocortical layer II/III pyramidal neurons from control and progenitor (Pg) *Lhx2* mutant groups.

(A) Traces showing voltage response to a 50-pA hyperpolarising pulse current for the example control (left) and Pg mutant (right) neurons. The resting membrane potential (V_{RMP}) is shown with a dotted line on top of the trace just before the current injection. Sag is represented as the difference between the initial peak and the steady-state voltage deflection. (B) Beeswarm plots of resting membrane potential (V_{RMP}) (left) and Sag ratio (right) recorded from all control and Pg mutant neurons. (C) Train of five excitatory postsynaptic potentials (α-EPSPs) recorded from example control (top) and Pg mutant (bottom) neurons. Temporal summation (S_α) was calculated as the ratio between the last and the first EPSP amplitudes. (D) Beeswarm of S_α recorded from all control and Pg mutant neurons. (E) *Top*, Chirp current stimulus. *Bottom*, Voltage responses of the example control and mutant neurons to the chirp current stimulus. (F–I) Beeswarm plots of maximum impedance amplitude (F), resonance frequency, f_R (G), resonance strength, Q (H), and total inductive phase, ϕ_L (I) calculated for all control and Pg mutant neurons. *Statistical test: Wilcoxon rank sum test. n represents the number of total neurons recorded in each group. The thick line on the right of each beeswarm plot depicts respective median values.*

Fig. S5

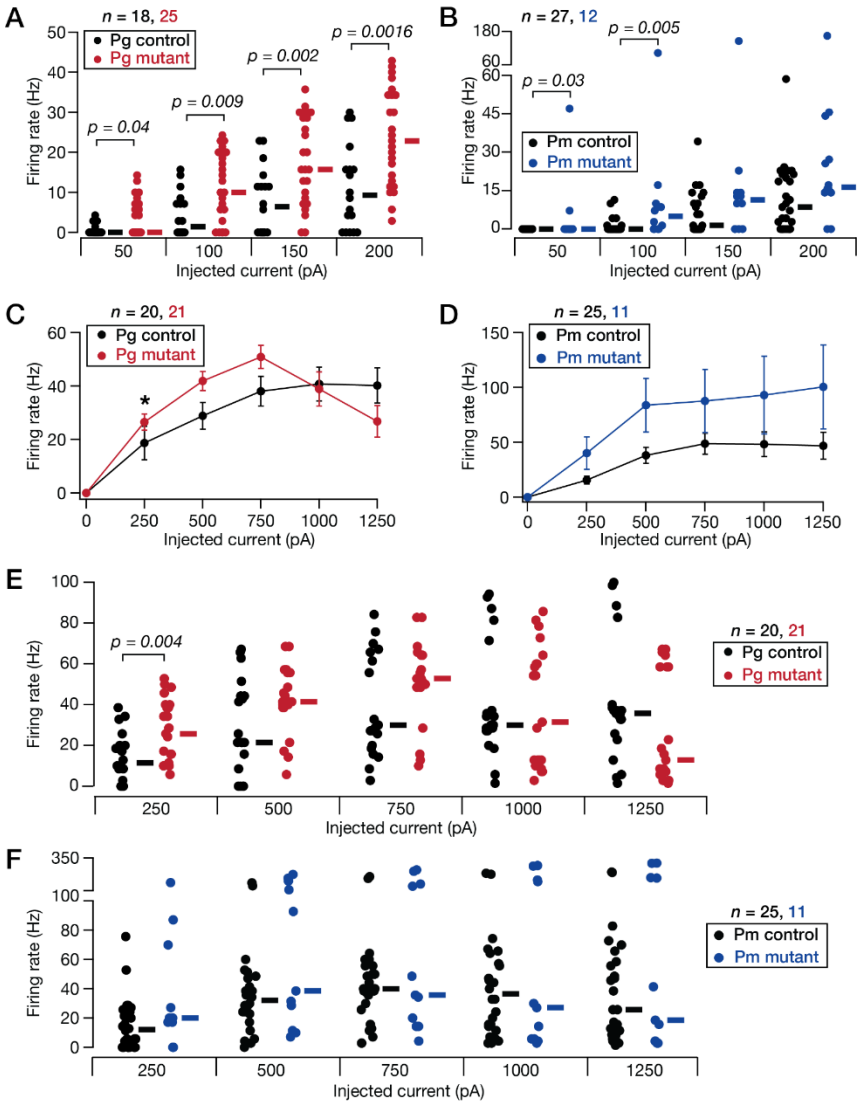

Supplementary Figure S5: Loss of *Lhx2* in progenitors (Pg) or postmitotic (Pm) neurons enhanced intrinsic excitability of neocortical layer II/III pyramidal neurons.

(A) Beeswarm plots of action potential firing frequencies for current injection amplitudes from 50–200 pA for control and Pg mutant neurons. (B) Same as panel A, for Pm mutant neurons and associated controls. (C) Mean-SEM plot showing firing rates of neurons from control and Pg mutant mice, plotted against current injection amplitudes from 250–1250 pA. (D) Same as panel C, for Pm mutant neurons and associated controls. (E) Beeswarm plots of action potential firing frequencies for current injection amplitudes from 250–1250 pA for control and Pg mutant neurons. (F) Same as panel E, for Pm mutant neurons and associated controls. *Statistical test: Wilcoxon rank sum test. n represents the number of total neurons recorded in each group. The thick line on the right of each beeswarm plot depicts respective median values.*

Fig. S6

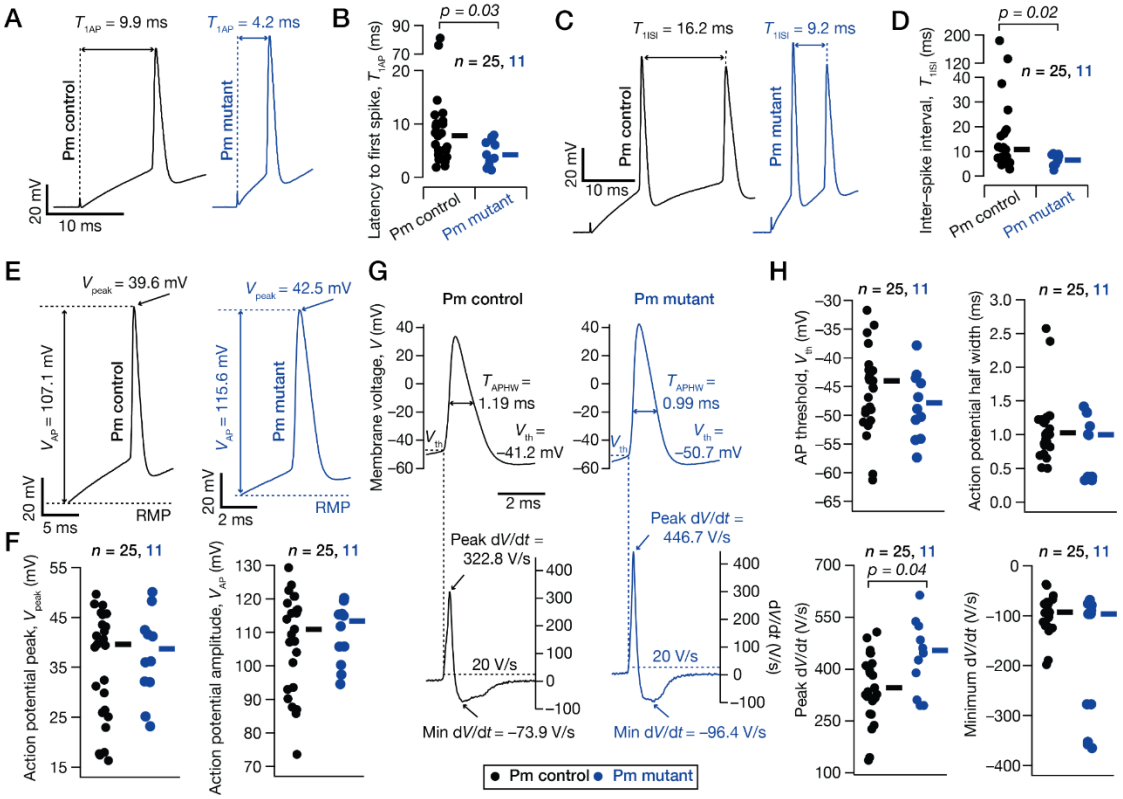

Supplementary Figure S6: Supra-threshold measurements for neocortical layer II/III pyramidal neurons from control and postmitotic (Pm) *Lhx2* mutant groups.

(A) The first action potential in a spike train, recorded in response to a 500-pA current injection into example neurons from control (left) and Pm mutant (right) groups. Arrows mark the latency to the first spike (T_{1AP}), measured from the start time of the current injection. (B) Beeswarm plot of T_{1AP} recorded from all control and Pm mutant neurons. (C) The first two action potentials in a spike train were recorded in response to a 500-pA current injection into example neurons from control (left) and Pm mutant (right) groups. Arrows mark the first inter-spike interval (T_{ISI}). (D) Beeswarm plot of T_{ISI} recorded from all control and Pm mutant neurons. (E) The first action potential in a spike train, recorded in response to a 500-pA current injection into example neurons from control (left) and Pm mutant (right) groups. The top arrow marks the peak voltage deflection V_{peak} . V_{AP} marks the action potential amplitude, measured from resting potential. (F) Beeswarm plots of V_{peak} and V_{AP} for control and Pm mutant groups. (G) The first action potential (top) in a spike train, recorded in response to a 500-pA current injection into example neurons from control (left) and Pm mutant (right) groups. The respective temporal derivatives (dV/dt) are shown below. Arrows mark the peak and the minimum dV/dt associated with each action potential. (H) Beeswarm plots of action potential threshold (V_{th}), action potential half-width (T_{APHW}), peak dV/dt, and minimum dV/dt from control and Pm mutant neurons. *Statistical test: Wilcoxon rank sum test. n represents the number of total neurons recorded in each group. The thick line on the right of each beeswarm plot depicts respective median values.*

Fig. S7

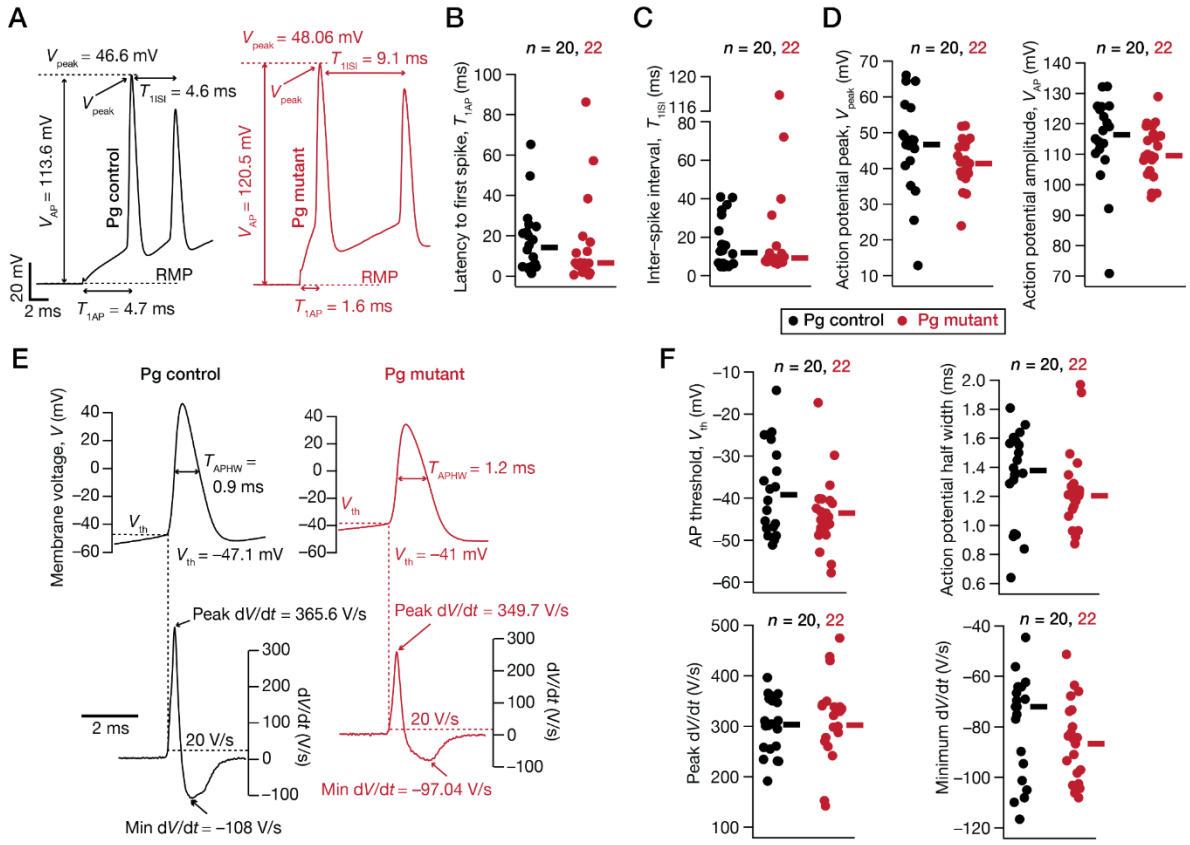

Supplementary Figure S7: Supra-threshold measurements for neocortical layer II/III pyramidal neurons from control and progenitor (Pg) *Lhx2* mutant groups.

(A) The first two action potentials in a spike train, recorded in response to a 500-pA current injection into example neurons from control (left) and Pg mutant (right) groups. Arrows mark the latency to the first spike (T_{1AP}), measured from the start time of the current injection, the first inter-spike interval (T_{ISI}). The top arrows mark the peak voltage deflection V_{peak}. V_{AP} marks the action potential amplitude, measured from resting membrane potential (RMP). (B) Beeswarm plot of recorded from all control and Pg mutant neurons. (C) Beeswarm plot of T_{ISI} recorded from all control and Pg mutant neurons. (D) Beeswarm plots of V_{peak} and V_{AP} for control and Pg mutant groups. (E) The first action potential (top) in a spike train, recorded in response to a 500-pA current injection into example neurons from control (left) and Pg mutant (right) groups. The respective temporal derivatives (dV/dt) are shown below. Arrows mark the peak and the minimum dV/dt associated with each action potential. (F) Beeswarm plots of action potential threshold (V_{th}), action potential half-width (T_{APHW}), peak dV/dt, and minimum dV/dt from control and Pg mutant neurons. *Statistical test: Wilcoxon rank sum test. n represents the number of total neurons recorded in each group. The thick line on the right of each beeswarm plot depicts respective median values.*

Fig. S8

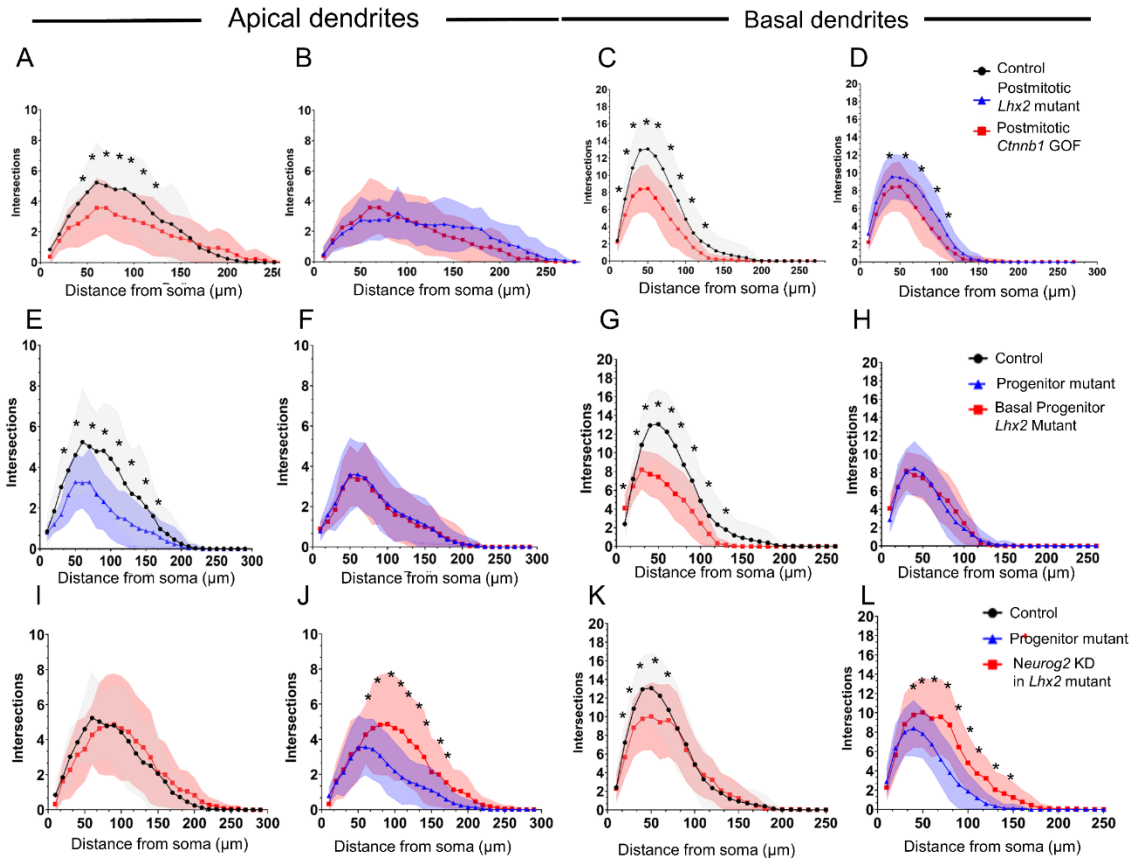

Supplementary Figure S8: Individual comparison of Sholl analysis from different conditions.

(A–D) Pairwise comparisons of apical (A, B) and basal (C, D) from Control, Pm mutant, and *Ctnnb1* GOF conditions as represented in Figure 5F, G. (E–H) Pairwise comparisons of apical (E, F) and basal (G, H) from Control, Pg mutant and *Eomes*-Cre driven basal progenitor mutant conditions as represented in Figure 4I, J. (E–H) Pairwise comparisons of apical (I, J) and basal (K, L) from Control, Pg mutant and *Neurog2* knockdown in *Lhx2* Pg mutant conditions as represented in Figure 4L, M. (30–40 neurons were analyzed from 3 biologically independent experiments. *Statistical test: Multiple T Tests (two-tailed). *(p<0.05).*

Fig. S9

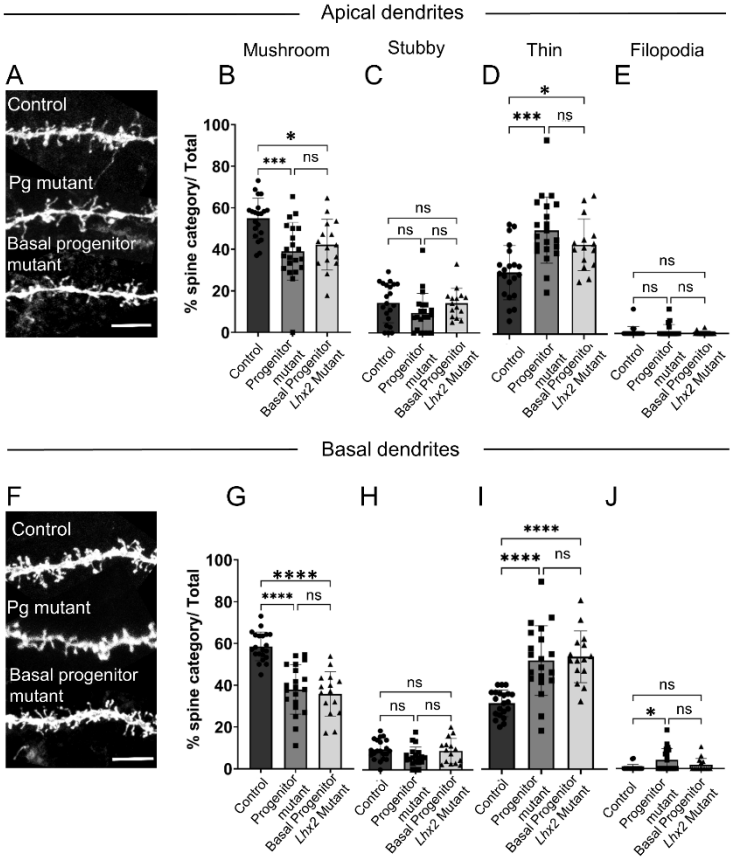

Supplementary Figure S9: Basal progenitor-specific *Lhx2* deletion recapitulates pan-progenitor-specific spine defects.

(A–J) Dendritic spine morphology is affected in *Eomes*-Cre-driven basal progenitor *Lhx2* mutant neurons. In apical and basal dendrites, the percentage of spines with mushroom morphology was significantly reduced (B, G) with a concomitant increase in thin morphology (D, I), similar to progenitor (Pg) mutants. The percentage of stubby spines was, however, not affected (C, H). The percentage of filopodial spines increased in Pg basal dendrites. 20 dendrites with 25 spines each were analysed from each category. *Statistical Test: Kruskal-Wallis Test*. *Scale bar: 5μm.*

Fig. S10

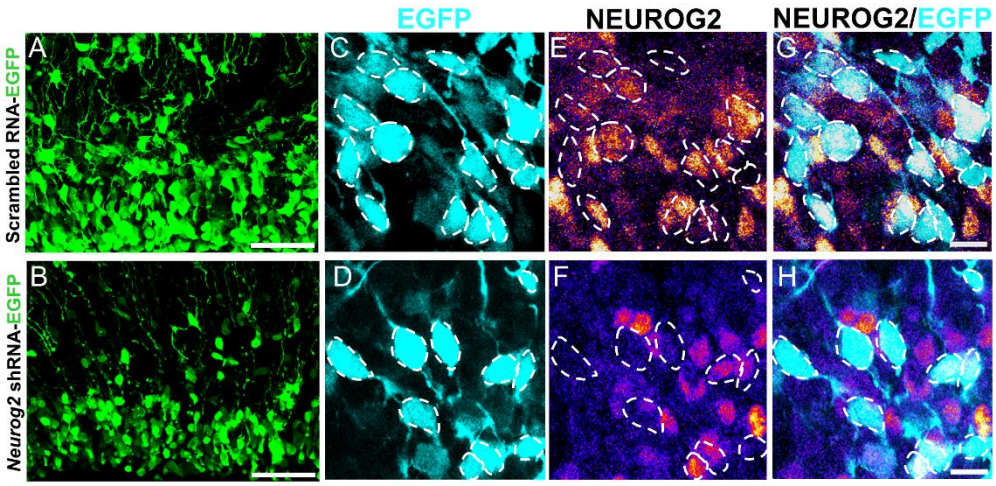

Supplementary Figure S10: *Neurog2* shRNA plasmid electroporation downregulates NEUROG2 expression. (A, B) Electroporation of scrambled pSilcaggs-scrambled RNA-EGFP (A) and pSilcaggs-*Neurog2* shRNA-EGFP (B) at E15.5 and analyzed at E16.5. Downregulation of *Neurog2* leads to delayed migration of cells (B), as previously described in (*36*). (C, D) *Neurog2* shRNA-EGFP (D) reduces NEUROG2 levels in electroporated cells compared to scrambled RNA (C). *N=2. Scale bars in (A, B) are 50μm, and (G, H) are 10μm.*

Data S1. (Separate file):

Statistical correlation of Sholl analysis for different datasets.

Sheet 1: Control vs Pg mutant vs Pm mutant Apical Dendrites (Figure 1H).

Sheet 2: Control vs Pg mutant vs Pm mutant Basal Dendrites (Figure 1I).

Sheet 3: Control vs Pm mutant vs Pm *Ctnnb1* GOF Apical Dendrites (Figure 3J).

Sheet 4: Control vs Pm mutant vs Pm *Ctnnb1* GOF Basal Dendrites (Figure 3K).

Sheet 5: Control vs Pg mutant vs *Eomes*-Cre *Lhx2* mutant Apical Dendrites (Figure 4K).

Sheet 6: Control vs Pg mutant vs *Eomes*-Cre *Lhx2* mutant Basal Dendrites (Figure 4L).

Sheet 7: Control vs Pg mutant vs *Neurog2* KD in *Lhx2* mutant Apical Dendrites (Figure 4N).

Sheet 8: Control vs Pg mutant vs *Neurog2* KD in *Lhx2* mutant Basal Dendrites (Figure 4O).

Data S2. (Separate file):

P5 Control versus Progenitor *Lhx2* mutant neuron RNA-Seq differentially expressed gene list.

Data S3. (Separate file):

P5 Control versus Postmitotic *Lhx2* mutant neuron RNA-Seq differentially expressed gene list.